Since January 2020 Elsevier has created a COVID-19 resource centre with free information in English and Mandarin on the novel coronavirus COVID-19. The COVID-19 resource centre is hosted on Elsevier Connect, the company's public news and information website.

Molecular Immunology 153 (2023) 160–169

Contents lists available at ScienceDirect

Molecular Immunology

journal homepage: www.elsevier.com/locate/molimm

Synergism of TNF-α and IFN-β triggers human airway epithelial cells death by apoptosis and pyroptosis

Rui Sun [a], Kaimin Jiang [a], Chengyue Zeng [a], Rui Zhu [b], Hanyu Chu [a], Huiyong Liu [a], Jingchun Du [a,c,1,*]

[a] Department of Clinical Immunology, Kingmed School of Laboratory Medicine, Guangzhou Medical University, Guangzhou, Guangdong 510182, China
[b] Department of Obstetrics and Gynecology, The First Affiliated Hospital of Guangzhou Medical University, Guangzhou, Guangdong 510120, China
[c] Guangzhou Key Laboratory of Clinical Rapid Diagnosis and Early Warning of Infectious Diseases, Guangzhou Medical University, Guangzhou, Guangdong 510182, China

ARTICLE INFO

Keywords:
TNF-α
IFN-β
Airway epithelial cells
Apoptosis
Pyroptosis

ABSTRACT

Cytokine release syndrome, also called cytokine storm, could cause lung tissue damage, acute respiratory distress syndrome (ARDS) and even death during SARS-CoV-2 infection. However, the underlying mechanisms of cytokine storm still remain unknown. Among these cytokines, the function of TNF-α and type I IFNs especially deserved further investigation. Here, we first found that TNF-α and IFN-β synergistically induced human airway epithelial cells BEAS-2B death. Mechanistically, the combination of TNF-α and IFN-β led to the activation of caspase-8 and caspase-3, which initiated BEAS-2B apoptosis. The activated caspase-8 and caspase-3 could further induce the cleavage and activation of gasdermin D (GSDMD) and gasdermin E (GSDME), which finally resulted in pro-inflammatory pyroptosis. The knock-down of caspase-8 and caspase-3 could effectively block the activation of GSDMD and GSDME, and then the death of BEAS-2B induced by TNF-α and IFN-β. In addition, pan-caspase inhibitor Z-VAD-FMK (ZVAD) and necrosulfonamide (NSA) could inhibit BEAS-2B death induced by TNF-α and IFN-β. Overall, our work revealed one possible mechanism that cytokine storm causes airway epithelial cells (AECs) damage and ARDS. These results indicated that blocking TNF-α and IFN-β-mediated AECs death may be a potential target to treat related viral infectious diseases, such as COVID-19.

1. Introduction

The ongoing global pandemic of coronavirus disease (COVID-19), caused by severe acute respiratory syndrome coronavirus 2 (SARS-CoV-2) has caused 535,248,141 confirmed cases, including 6,313,229 deaths (WHO, 2022). Characterization of histopathology and cellular localization of SARS-CoV-2 in the tissues of patients with fatal COVID-19 confirmed that SARS-CoV-2 mainly infected upper and lower airways epithelial cells, type 2 pneumocytes, and endothelial cells, which resulted in tracheobronchitis, diffuse alveolar damage (DAD) and vascular injury. As the first defense line, airway epithelial cells were first infected and attacked by SARS-CoV-2. So, respiratory mucosal ulceration and pathologic injury mixed with inflammatory cell infiltration were the classic traits of COVID-19 (Borczuk et al., 2020; Martines et al., 2020). However, the molecular mechanism employed by SARS-CoV-2 to destroy respiratory mucosal epithelium still remains unclarified.

At present, plenty of evidence indicated that COVID-19 mainly was fatal to elderly adults, which may be related to severe systemic elevation of several pro-inflammatory cytokines and then induced cytokine storm (Meftahi et al., 2020). Several studies reported that serum levels of pro-inflammatory cytokines, such as IFN-α, IFN-γ, IL-1β, IL-6, TNF-α, GM-CSF, IP10, C-reactive protein (CRP) et al., were markedly increased in patients with severe COVID-19 (Huang et al., 2020; Karki et al., 2021; Meftahi et al., 2020; Wang et al., 2020). Among these cytokines, the function of TNF-α and type I IFNs especially deserved further investigation (Lee and Shin, 2020). TNF-α is an important inflammatory cytokine, which promotes homeostasis by regulating inflammation, cell proliferation, differentiation, survival, and death in response to infection (Chen and Goeddel, 2002; Walczak, 2011). In general, TNF-α induces the formation of Complex I through its membrane receptor

* Corresponding author at: Department of Clinical Immunology, Kingmed School of Laboratory Medicine, Guangzhou Medical University, Guangzhou, Guangdong 510182, China.
E-mail address: hnxydjc@gzhmu.edu.cn (J. Du).
[1] ORCID ID: http://orcid.org/0000-0002-0571-7444

https://doi.org/10.1016/j.molimm.2022.12.002
Received 21 June 2022; Received in revised form 19 October 2022; Accepted 3 December 2022
Available online 9 December 2022

TNFR1, which activates NF-κB signaling and benefits cell survival (Silke, 2011). However, under certain conditions Complex I is dissociated to form Complex II, which could lead to apoptosis by activating caspase-8, or necroptosis mediated by RIPK3 (receptor-interacting protein kinase 3) and MLKL (mixed lineage kinase-like protein) (Pasparakis and Vandenabeele, 2015). Excessive or continuous involvement of TNF-α during infection, ischemia, or trauma could cause inflammatory disease, such as SIRS (systematic inflammatory response syndrome), and during which type I IFNs act as essential mediators in TNF-induced lethal inflammatory shock, possibly by enhancing cell death and inducing chemokines and WBCs (white blood cells) infiltration in tissues (Huys et al., 2009; Tracey et al., 1986). Based on present studies, we hypothesized that TNF-α and type I IFNs might mediate the destroy of respiratory mucosal epithelium during COVID-19.

Here, we modeled the effect of pro-inflammatory cytokines on human airway epithelial cells by culturing human airway epithelial cells BEAS-2B under different combinations of cytokines and first reported that TNF-α and IFN-β synergistically induced BEAS-2B death. Mechanistically, the co-treatment of TNF-α and IFN-β triggered BEAS-2B death by apoptotic and pyroptotic, not necroptotic pathway. In addition, pan-caspase inhibitor Z-VAD-FMK (ZVAD) and necrosulfonamide (NSA) could inhibit BEAS-2B death induced by TNF-α and IFN-β. Our findings may provide new insight to treat related viral infection and diseases, such as COVID-19.

2. Materials and methods

2.1. Cell culture

BEAS-2B, 16HBE, H1975, and HT29 cells were obtained from the ATCC and routinely cultured in Dulbecco's Modified Eagle's Medium (DMEM) supplemented with 10% fetal bovine serum (FBS), penicillin (100 U/ml) and streptomycin (100 μg/ml) in a 37 °C humidified incubator containing 5% CO2. All the cell lines were validated by short tandem repeat profiling analysis and were free of mycoplasma contamination.

2.2. Reagents

The following reagents were used: TNF-α (T, Novoprotein, Fremont, CA), IFN-β (Peprotech, Rocky Hill, NJ), IFN-γ (Novoprotein, Fremont, CA), Z-VAD-FMK (Z, ZVAD), Z-DEVD-FMK, Z-IETD-FMK, Smac-mimetic (S), GSK-872 and necrosulfonamide (NSA). All small molecular chemical compounds were provided by MCE, Shanghai, China. The compouds ZVAD, Z-DEVD-FMK, Z-IETD-FMK, S, GSK-872 and NSA were used at concentration of 20 μM, 20 μM, 10 μM, 100 nM, 10 μM and 5 μM, respectively. Antibodies against Caspase-8, Caspase-3, PARP1, RIPK3, pMLKL, MLKL, β-Actin, and GAPDH were purchased from Cell Signaling Technology, and antibodies against Caspase-1, GSDMD and GSDME were obtained from Abcam.

2.3. Cellular viability and death assays

Cells were plated in a 96-well plate (4×10^4 cells/ml) and treated with different combinations of TNF-α and type I/II IFNs with or without compounds for 72 h or TS for 3 h as indicated. Next, cell viability was analyzed by the CellTiter-Glo Luminescent Cell Viability Assay kit (Promega, Madison, WI), and cell death was determined by the Cytotoxicity LDH Assay kit (Dojindo, Kumamoto, Japan) according to the manufacturer's instructions. Luminescence and absorbance were measured using a Microplate Reader (Bio-Rad, Hercules, CA). The results were shown as the ratio against the untreated control group, respectively.

To directly observe cell death, cells plated in 96-well plates (4×10^4 cells/ml) were treated as mentioned above, and then stained with Annexin V-FITC and PI (Sungene Biotech, Tianjin China), or nucleic acid dye SYTOX Green (Promega, Madison, WI) and DAPI (Sigma-Aldrich, St. Louis, MO) according to the manufacturer's instructions. To quantify the difference between each group, the ratio of positive cells were analyzed based on 10 high power fields (HPF, 200x).

2.4. Western blot analysis

After being treated as indicated, the cells were washed twice with cold PBS buffer, scraped, and lysed with lysis buffer (100 μl RIPA lysis buffer supplemented with protease and phosphatase inhibitors) to extract the whole protein. Protein concentration was determined by BCA Protein Assay Kit (Bio-rad) according to the manufacturer's protocol. Cell lysates were separated by electrophoresis on SDS- PAGE gel and then transferred to PVDF (Millipore, Billerica, MA). The membranes were blocked with 5% skimmed milk in phosphate buffer containing 0.1% Tween-20 (PBST) for 30 min at room temperature, and incubated with primary antibodies specific for PARP1 (1:1000), Caspase-1 (1:1000), Caspase-8 (1:1000), Caspase-3 (1:1000), GSDME (1:1000), GSDMD (1:1000), RIPK3 (1:1000), pMLKL (1:1000), MLKL (1:1000), β-Actin(1:2000) or GAPDH (1:2000) at 4 °C overnight. After washed, the membranes were incubated with HRP-conjugated secondary antibodies at room temperature for 2 h, then detected using a chemiluminescence signaling detection kit (CST, Beverly, MA).

2.5. Immunofluorescence

Cells were fixed with 4% paraformaldehyde and then permeated with 0.3% Triton X-100. After blocking with 5% normal goat serum for 1 h, the cells were incubated with the primary antibody of active-Caspase3 (Promega, Madison, WI) diluted at 1:300 overnight at 4 °C, and then incubated with the Cy3-coupled secondary antibody (Abcam) diluted at 1:500 for 1 h at room temperature and protected from light. Cells were stained with DAPI according to the manufacturer's instructions, and the staining results were recorded and analyzed with Cell Imaging Multi-Mode Reader (BioTek, Winooski, VT).

2.6. Knock-down of caspase-8 and caspase-3

Gene-specific targeting oligos were cloned into the LentiCRISPR V2 vector (Addgene 52961), which was co-transfected with pMD2.G (Addgene 12259) and psPAX2 (Addgene 12260) into 293 T cells to produce lentiviruses. BEAS-2B were transduced with the viruses, and then were selected with 0.5 μg/ml puromycin and/or 50 μg/ml hygromycin. After two turns of selection, the pool cells were used for the followed assay. The following targeting sequences were used. Caspase-8, ATGATCAGACAGTATCCCCG and CAAATGAAAAGCAAACCTCG; Caspase-3,

CAAGGAATGACATCTCGGTC and ATGTCGATGCAGCAAACCTC.

2.7. ELISA

The supernatant media derived from the untreated control, BEAS-2B treated with TNF-α and IFN-β for 24 h and 48 h, were collected, and the concentration of IL-1β in which was measured using a human IL-1β ELISA kit (Neobioscience, Shenzhen, China), according to the instructions of the manufacturer.

2.8. Statistical analysis

All experiments were representative of three or more experiments. GraphPad Prism version 9.0 software was used for graph formation and data analysis. All quantitative data were shown as mean ± SEM. Statistical significance was determined by t test (two-tailed) for two groups or one-way ANOVA for three or more groups. Statistical significance was determined with: *P < 0.05; * *P < 0.01; * **P < 0.001; * ** *P < 0.0001; ns, not significant.

3. Results

3.1. TNF-α and IFN-β synergistically affect airway epithelial cells growth and death

To investigate which kind of cytokine affect airway epithelial cells growth, we first treated human airway epithelial cells BEAS-2B with different concentration of TNF-α, IFN-β, and IFN-γ, respectively, and found that all three kinds of cytokine had some degree of inhibitory effect on cell growth, while the effect of IFN-β was the most significant among the detected cytokines (Fig. 1A). Next, the different combinations of three cytokines were used to treat BEAS-2B and we found that the combination of TNF-α and IFN-β significantly reduced cell viability and it seemed that IFN-γ lack the synergic effect with TNF-α and IFN-β (Fig. 1B). These results suggested that TNF-α and IFN-β had a synergistic effect on inhibiting cell growth. To further make sure the effect of cytokine concentration on cell survival, BEAS-2B were then treated with different concentration of TNF-α and IFN-β as indicated. The results indicated that the concentration of TNF-α in 20 ng/ml & 40 ng/ml had little difference on effect of cell survival, while the concentration of IFN-β had dramatically effect on cell survival and the inhibitory effect was concentration- dependent (Fig. 1C). So the concentration of all cytokines we used in the following experiments was 20 ng/ml. Moreover, the inhibitory effect of TNF-α and IFN-β was also time-dependent (Fig. 1D).

On the other hand, the morphology change of BEAS-2B treated with TNF-α and IFN-β was observed and the characteristics of cell death phenomena, including a reduction in the extent of cell-cell adherence and the appearance of cellular debris, were very obvious (Fig. 2A). To further understand the cell death, BEAS-2B treated with TNF-α and IFN-β were stained with SYTOX Green/DAPI and a large number of fluorescein-binding dying cells were observed when IFN-β was used alone, and more dying cells were observed when IFN-β was used in combination with TNF-α (Fig. 2B). As shown in Fig. 2C, the percentage of SYTOX Green positive cells were significantly higher in cytokines-treated BEAS-2B than those in control. In addition, the LDH levels in supernatant media were significantly increased after BEAS-2B was treated with TNF-α and IFN-β (Fig. 2D), which further confirmed the cytotoxic effect of TNF-α and IFN-β. These results indicated that cell membrane damage and cell death had occurred in TNF-α and IFN-β co-treated BEAS-2B. At the same time, TNF-α combined with IFN-β also significantly reduced the survival of another two lung tissue-derived cell lines 16HBE and H1975 cells (Fig. 2E). So it may be a common phenomenon that TNF-α and IFN-β synergistically damage airway epithelial cells. Taken together, these findings revealed that TNF-α enhances IFN-β -induced airway epithelial cells death.

3.2. TNF-α and IFN-β induced apoptosis of BEAS-2B

To understand how TNF-α and IFN-β induce cell death in BEAS-2B, special compound inhibitors including broad-spectrum caspase inhibitor ZVAD, RIPK3 inhibitor GSK-872, and MLKL inhibitor NSA, were first used to identify possible programmed cell death pathway. The results indicated that both ZVAD and NSA, not GSK-872, could partially inhibit TNF-α/IFN-β-induced cell death (Fig. 3A), which prompted that BEAS-2B might happen apoptosis and necroptosis after treatment with TNF-α and IFN-β. The appearance of Annexin V-FITC/PI double-positive cells after co-treatment with TNF-α and IFN-β further intensified our hypothesis (Fig. 3B). To confirm the apoptosis of BEAS-2B treated with TNF-α and IFN-β, the activation of caspase-3 was first detected by immunofluorescence staining and the activated caspase-3 was observed when IFN-β was used alone, and the activation of caspase-3 was more pronounced when TNF-α was combined with IFN-β (Fig. 3C&D), which

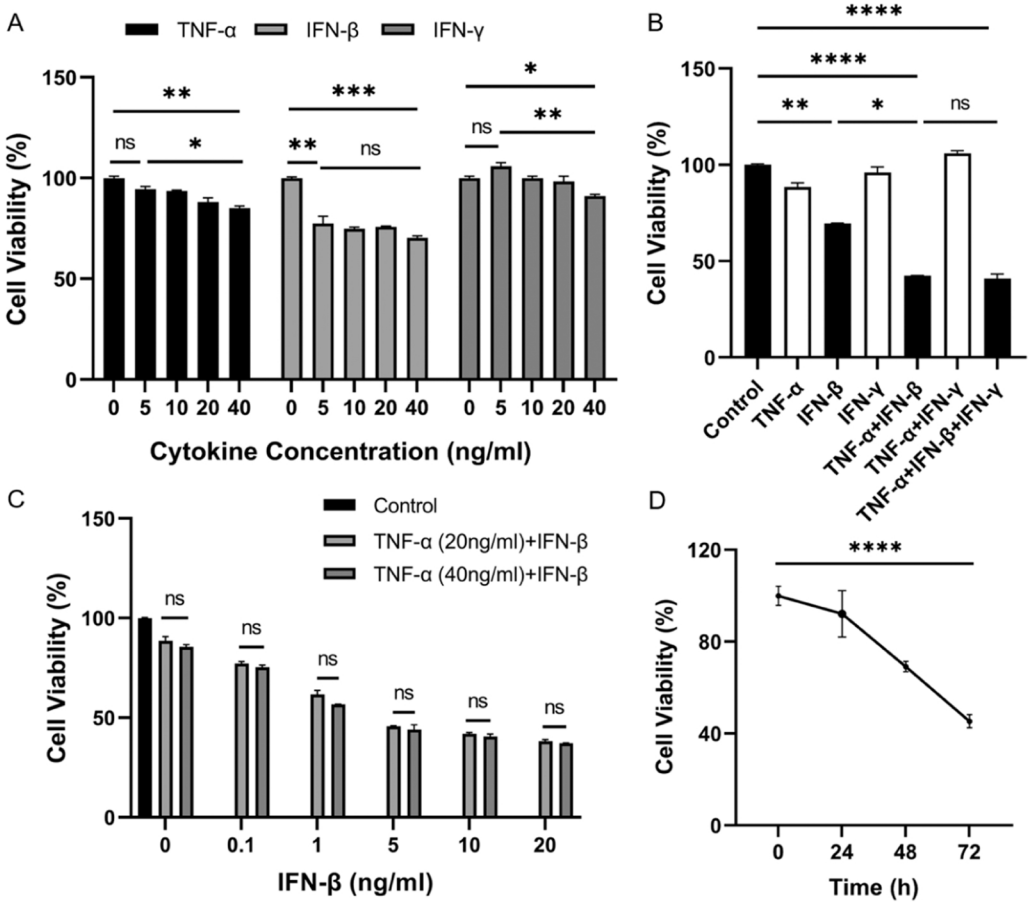

Fig. 1. TNF-α and IFN-β synergistically inhibit human airway epithelial cells growth. The cell viability of BEAS-2B was detected after cells were treated with different concentration of TNF-α, IFN-β, and IFN-γ as indicated for 72 h (**A**), different combinations of TNF-α, IFN-β and IFN-γ (20 ng/ml of each cytokine) for 72 h (**B**), different concentrations of IFN-β as indicated for 72 h under two concentrations of TNF-α (**C**), TNF-α and IFN-β (20 ng/ml of each cytokine) for 24, 48 and 72 h, respectively (**D**). The results are representative of at least three separate experiments. All data are shown as mean ± SEM. * $p < 0.05$, * * $p < 0.01$, * ** $p < 0.001$, * ** * $p < 0.0001$, ns, not significant. All analysis was performed using the one-way ANOVA.

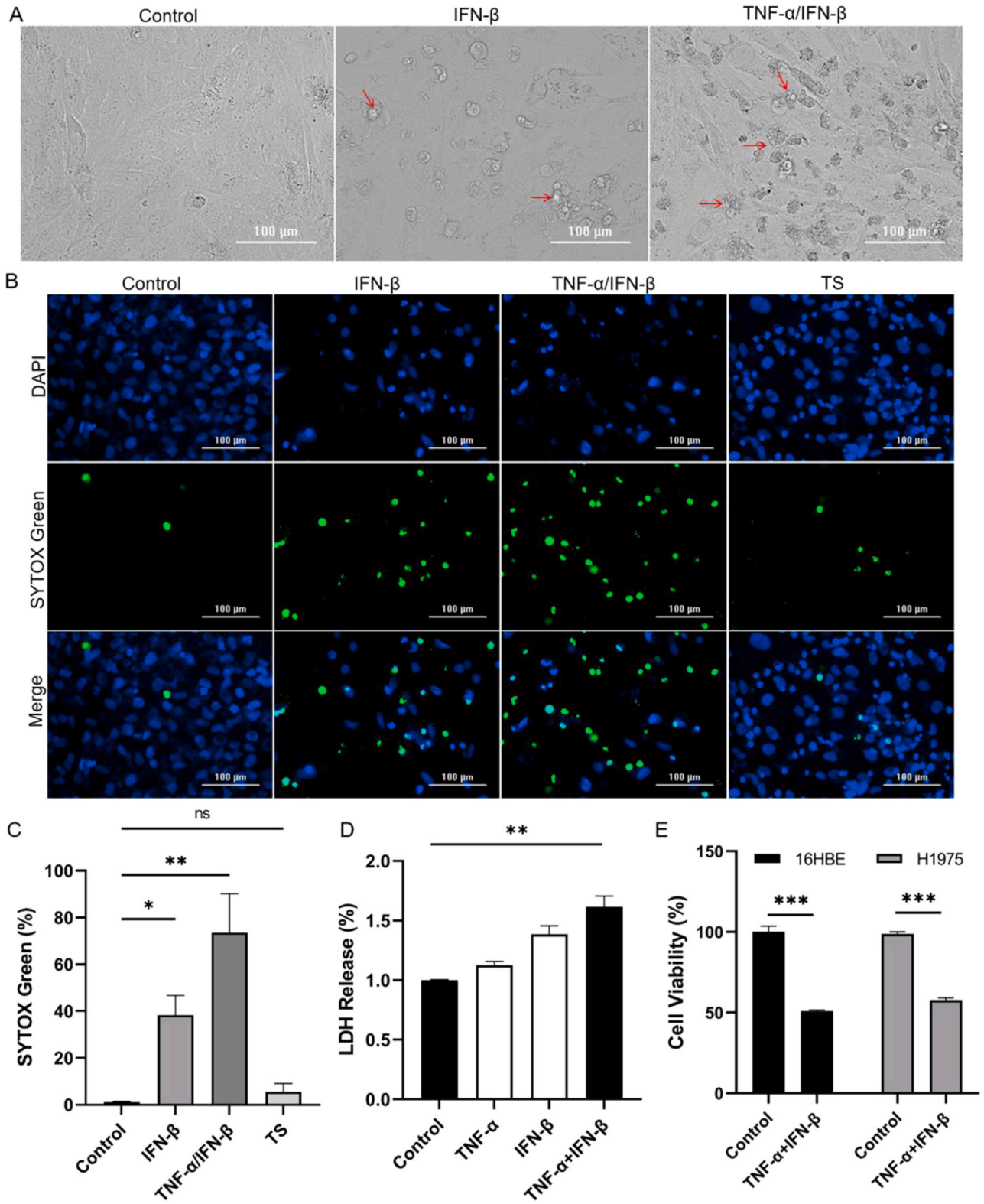

Fig. 2. TNF-α and IFN-β synergistically induce human airway epithelial cells death. **(A)** Representative light microscopy images of BEAS-2B after cells were treated with IFN-β alone or combined with TNF-α for 72 h. The typical dead cells were marked with arrow. **(B)** Representative fluorescence microscope images of BEAS-2B after cells were treated with IFN-β alone or combined with TNF-α for 72 h, and TS for 3 h. Green fluorescence represented dead cells and blue fluorescence represented total cells. Scale bar, 100 μm. **(C)** The difference of SYTOX Green-positive cells between control and treated groups were quantified. **(D)** The LDH released from cells was measured after BEAS-2B cells were treated as indicated for 72 h. **(E)** The cell viability was detected after 16HBE and H1975 cells were treated with TNF-α and IFN-β for 72 h, respectively. The results are representative of at least three separate experiments. Data are shown as mean ± SEM **(C-E)**. * *$p < 0.01$, * ** $p < 0.001$, ns, not significant. Analysis was performed using the one-way ANOVA **(C&D)** or the t test **(E)**.

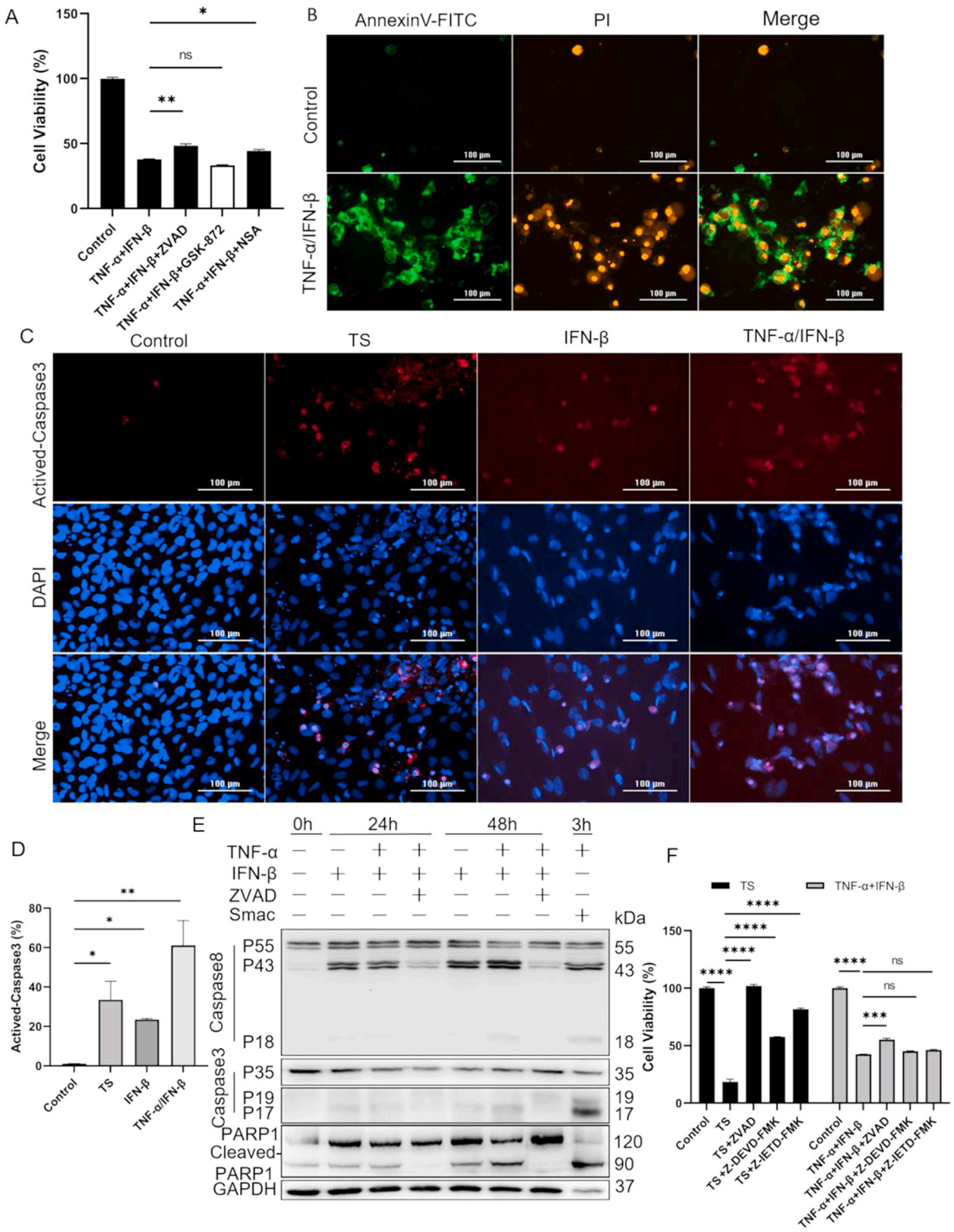

Fig. 3. TNF-α and IFN-β synergistically induce apoptosis of BEAS-2B. **(A)** The inhibitory effect of specific compounds on BEAS-2B death induced by TNF-α and IFN-β were detected by cell viability assay. **(B)** BEAS-2B cells were treated with TNF-α and IFN-β for 72 h followed by Annexin V-FITC and PI staining. **(C)** The active-caspase-3 in BEAS-2B were detected by IF staining after cells were treated with TS for 3 h, and IFN-β alone or combined with TNF-α for 72 h. **(D)** The difference of activated caspase-3 between control and treated groups were quantified. **(E)** The cleavage and activation of caspase-8, caspase-3, and PARP1 were analyzed by western blot after BEAS-2B was treated as indicated for 24 and 48 h, respectively. **(F)** The cell death pathways of BEAS-2B induced by TS and TNF-α/IFN-β were compared using specific compound inhibitors as indicated. The results are representative of at least three separate experiments. Data are shown as mean ± SEM. * $p < 0.05$, * * $p < 0.01$, * ** $p < 0.001$, * ** * $p < 0.0001$, ns, not significant. Analysis was performed using the one-way ANOVA.

indicated that TNF-α and IFN-β synergistically induced apoptosis in BEAS-2B. Then, the western blot was used to further confirm the occurrence of apoptosis in BEAS-2B, the results indicated that caspase-8, caspase-3, and PARP1 were activated in both IFN-β and TNF-α/IFN-β treated cells and the activation of these effector molecules showed dramatically time-dependent. Moreover, IFN-β combined with TNF-α could more effectively activate caspase-8, caspase-3, and PARP1 compared to IFN-β alone, and ZVAD could inhibit the activation of these effector molecules induced by TNF-α and IFN-β (Fig. 3E). So, it could be concluded that apoptosis was truly occurred in BEAS-2B after treatment with TNF-α and IFN-β.

In addition, the broad-spectrum caspase inhibitor ZVAD, caspase-3 inhibitor Z-DEVD-FMK and caspase-8 inhibitor Z-IETD-FMK were used to explore whether TNF-α and IFN-β induced other forms of cell death pathways besides apoptosis by comparing cell survival of BEAS-2B after treatment with TNF-α/IFN-β for 72 h and TNF-α/Smac-mimetic (T/S) for 24 h, respectively. The results indicated that caspase inhibitors could almost completely inhibit T/S-induced cell death, but not TNF-α/IFN-β-induced cell death, suggesting that the cell death pathways induced by T/S and TNF-α/IFN-β were not completely same, and TNF-α/IFN-β should also induce other form of cell death besides apoptosis (Fig. 3F).

3.3. TNF-α and IFN-β could not induce necroptosis of BEAS-2B

To investigate whether TNF-α and IFN-β could induce necroptosis of BEAS-2B, GSK-872 (RIPK3 inhibitor), and NSA (MLKL inhibitor) were used to inhibit TNF-α/IFN-β-induced cell death under the condition that caspase-8 activity was blocked with ZVAD. The results indicated that NSA, not GSK-872, could partially inhibit TNF-α/IFN-β-induced cell death when caspase-8 activity was deficient, which was also intensified by the immunofluorescence staining results (Fig. 4A-C). But because GSK-872 and NSA did not consistently function inhibitory effect on cell death compared to control treated with TNF-α and IFN-β (Fig. 4A), whether TNF-α and IFN-β synergistically induced necroptosis of BEAS-2B deserved further investigation. First, the phosphorylated and total MLKL (executor of necroptosis) were detected and the results indicated that IFN-β and TNF-α/IFN-β just increased the expression of MLKL, and all combinational treatment did not induce phosphorylated MLKL in BEAS-2B (Fig. 4D). Secondly, the expression of RIPK3 was then detected, and the result indicated that RIPK3 was not expressed in BEAS-2B though it was expressed in HT29 (Fig. 4E). In general, the phosphorylation and activation of MLKL occur downstream of activation of protein kinases RIPK3, one key effect molecule of necroptosis, during happening of necroptosis (Pasparakis and Vandenabeele, 2015). Together, these findings explained why activated MLKL was deficient in

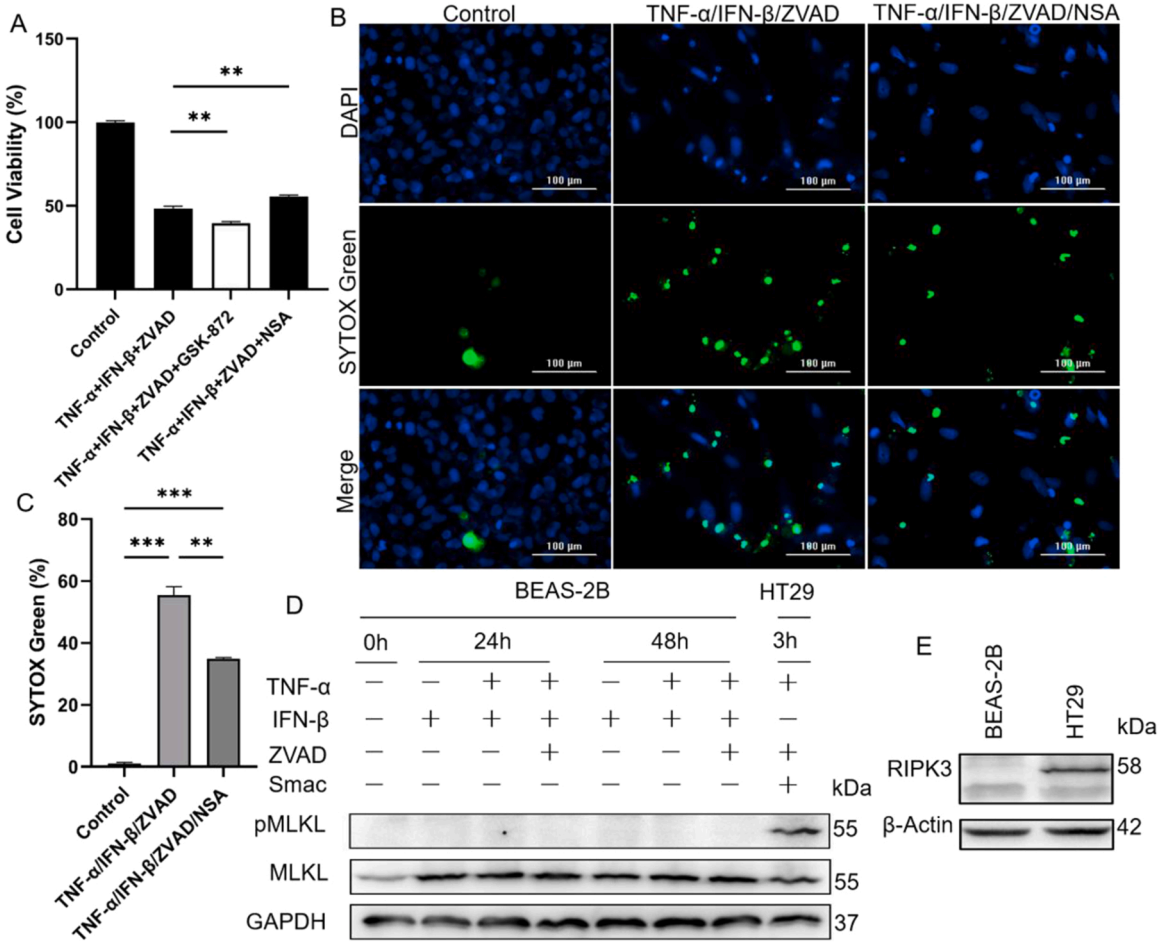

Fig. 4. TNF-α and IFN-β could not cause necroptosis of BEAS-2B. **(A)** The blocking effect of inhibitor GSK-872 and NSA on BEAS-2B death induced by TNF-α and IFN-β were detected under condition that enzymatic activity of caspase-8 was inhibited by ZVAD. **(B)** Representative fluorescence microscope images of BEAS-2B after treated with cytokines and inhibitors as indicated for 72 h. Green fluorescence represented dead cells and blue fluorescence represented total cells. Scale bar, 100 μm. **(C)** The difference of SYTOX Green-positive cells between control and treated groups were quantified. **(D)** The phosphorylated MLKL and total MLKL were analyzed by western blot after BEAS-2B were treated for 24 and 48 h with different combinations of cytokines and inhibitors as indicated. TSZ-treated HT29 was as a control. **(E)** The expression of RIPK3 in BEAS-2B and HT29 were analyzed by western blot. The results are representative of at least three separate experiments. Data are shown as mean ± SEM. * * $p < 0.01$, * ** $p < 0.001$. Analysis was performed using the one-way ANOVA.

TNF-α/IFN-β-treated BEAS-2B and demonstrated that TNF-α and IFN-β did not induce necroptosis of BEAS-2B.

3.4. TNF-α and IFN-β induced pyroptosis of BEAS-2B by activating GSDMD and GSDME

Pyroptosis is one form of pro-inflammatory cell death pathway and

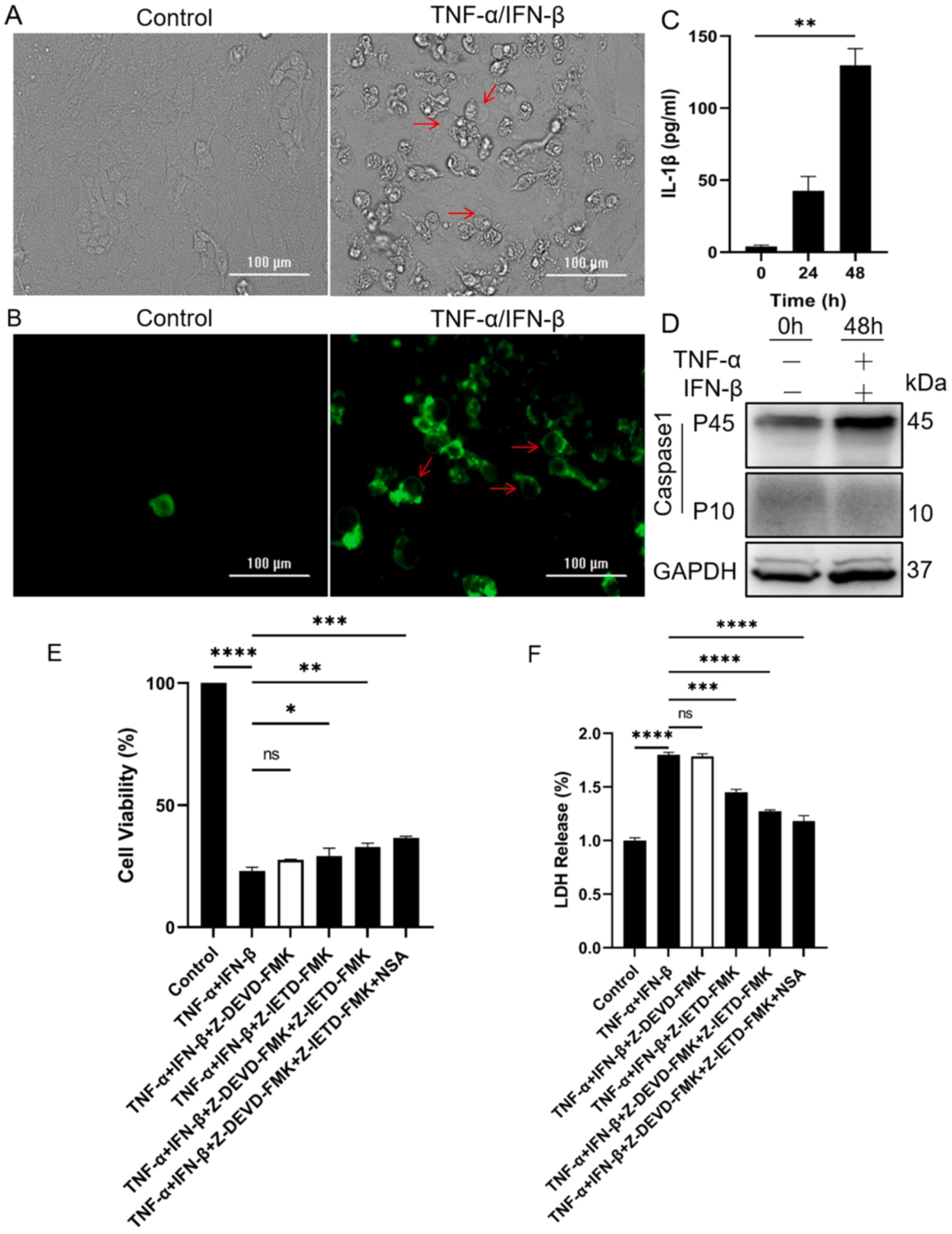

Fig. 5. TNF-α and IFN-β synergistically induce BEAS-2B death in a manner similar to pyroptosis. **(A&B)** Representative light and fluorescence microscopy images of BEAS-2B after treated with TNF-α and IFN-β for 72 h. The green fluorescence indicates Annexin V-FITC positive. Scale bar, 100 μm. **(C)** The concentration of IL-1β in supernatant media was assayed by ELISA, after BEAS-2B were treated with TNF-α and IFN-β. **(D)** The cleaved and full length fragment of caspase-1 was assayed by western blot, after BEAS-2B were treated as indicated. The cell viability **(E)** and LDH release **(F)** of BEAS-2B were determined after cells were treated as indicated for 72 h. The results are representative of at least three separate experiments. Data are shown as mean ± SEM. * $p < 0.05$, * * $p < 0.01$, * ** $p < 0.001$, * ** * $p < 0.0001$, ns, not significant. Analysis was performed using the one-way ANOVA.

depends on caspase-mediated cleavage and activation of gasdermin family proteins (GSDMs), which eventually leads to cell membrane rupture and the release of cytoplasmic contents, such as IL-1β. During the processing of pyroptosis, cells commonly show typical morphological changes, including plasma membrane swelling and bubble-like bulging. It was amazing that the typical morphological characteristics of pyroptotic cells also appeared in TNF-α/IFN-β-treated BEAS-2B (Fig. 5A&B). At the same time, there existed the release of IL-1β after BEAS-2B were treated with TNF-α and IFN-β (Fig. 5C). It was reported that activated caspase-1, caspase-8 and caspase-3 could initiate pyroptosis by cleaving GSDMD and GSDME, respectively (Sarhan et al., 2018; Wang et al., 2017). So the activation of caspase-1 was first detected, the results indicated that TNF-α and IFN-β did not induce the activation of caspase-1 in BEAS-2B (Fig. 5D). To confirm whether TNF-α and IFN-β could induce pyroptosis of BEAS-2B by caspase-3/8-mediated pathway, caspase-3 inhibitor Z-DEVD-FMK and caspase-8 inhibitor Z-IETD-FMK with or without NSA were used to block cell death induced by TNF-α and IFN-β, the results indicated that combination of caspase-3 inhibitor and caspase-8 inhibitor could partially improve cell survival and reduce LDH release (Fig. 5E&F). Because of the possible off-target effect of small molecular inhibitor, and to further identify the activation role of caspase-8 and caspase-3 on GSDMD and GSDME, the expression of caspase-8 and caspase-3 were separately or simultaneously knocked down (Fig. 6A&B). The expression decline of caspase-8 and caspase-3 obviously relieved the cytotoxic effect of TNF-α and IFN-β on BEAS-2B (Fig. 6C), and correspondingly caused the decline of activated GSDMD and GSDME (Fig. 6D&E).

To further investigate whether ZVAD and NSA could co-operate to block the cytotoxic effect of TNF-α and IFN-β on BEAS-2B, the expression and activation of GSDMD and GSDME were first examined, and the results indicated that ZVAD could obviously decline the cytotoxic cutting-fragment of GSDMD and GSDME induced by TNF-α and IFN-β (Fig. 7A). NSA could co-operate with ZVAD to inhibit the activation of GSDMD and GSDME by non-directly blocking the activation of caspase-8 and caspase-3 (Fig. 7B-D). On the other hand, when the activation of caspase-8 and caspase-3 induced by TNF-α and IFN-β were inhibited by ZVAD, the activation of GSDMD and GSDME were correspondingly attenuated (Fig. 7D). Taken together, these results indicated that TNF-α and IFN-β induced the cleavage and activation of GSDMD and GSDME in BEAS-2B cells by activating caspase-8 and caspase-3, which finally resulted in the happening of pyroptosis, and ZVAD and NSA could co-operate to block this cytotoxic effect of TNF-α and IFN-β.

4. Discussion

Present reports have shown that cytokine storm rather than a direct damage effect of the virus itself plays a key important role in pneumonia, ARDS and multi-organ dysfunction caused by SARS-CoV-2 infection (Lucas et al., 2020; Mehta et al., 2020). However, the concrete pro-inflammatory cytokines those played a determinant role in COVID-19 still remain incompletely clear. At the same time, different cytokines may function different role in inducing different forms of cell death and tissue damage. For example, the combination of TNF-α and IFN-γ could induce inflammatory cell macrophage death, and then inflammation, tissue and organ damage (Karki et al., 2021). Type I IFNs could restrict SARS-CoV-2 infection of human airway epithelial cultures, but it seems that type I IFNs also exacerbated TNF-α and IL-1-drived inflammation in the progression to severe COVID-19 (Lee et al., 2020; Vanderheiden et al., 2020). Furthermore, type I IFNs could disrupt lung epithelial repair during recovery from influenza viral infection by directly reducing p53-mediated epithelial proliferation and differentiation (Major et al., 2020). These reports indicated that the effect of type I IFNs on airway epithelial cells was complex and the related molecular mechanism was not completely clear.

Our study first suggested that IFN-β could inhibit proliferation and induce death of human airway epithelial cells BEAS-2B, and TNF-α exacerbated this effect (Fig. 1&2). The morphological change of cells and release of a large amount of LDH indicated that BEAS-2B treated with TNF-α and IFN-β might undergo not only non-proinflammatory cell death but also pro-inflammatory cell death (Fig. 2). It was reported that the combinations of TNF-α and type I IFNs signaling pathways mediated the co-occurrence of apoptosis and necroptosis, leading to perinatal death in RIPK1-deficient mice (Kaiser et al., 2014). Next, we made sure whether the combination of TNF-α and IFN-β could induce apoptosis and necroptosis in BEAS-2B and found that broad-spectrum caspase inhibitor ZVAD and NSA, not RIPK3 inhibitor GSK-872, could block cell death induced by TNF-α and IFN-β, respectively (Fig. 3A). The Annexin V-FITC was positive and a large amount of activated caspase-3 was detected in BEAS-2B treated with TNF-α and IFN-β, which confirmed the occurrence of apoptosis, but could not confirm whether there was an occurrence of necroptosis in this progression (Fig. 3B-D). Moreover, as we traced further, the activated fragments of caspase-8, caspase-3, and PARP1 were detected, and the specific compound inhibitors blocked the activation of these effector molecules, all these results proved the occurrence of apoptosis in BEAS-2B treated with TNF-α and IFN-β (Fig. 3E). Interestingly, the death of BEAS-2B induced by TNF-α and IFN-β could

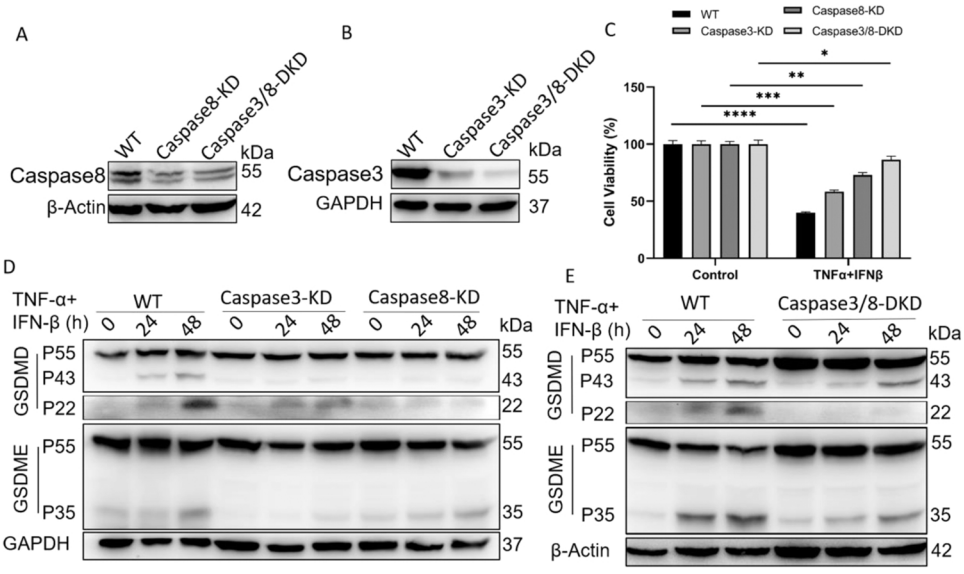

Fig. 6. Knock-down of caspase-8 and caspase-3 relieve the cytotoxic effect of TNF-α and IFN-β on BEAS-2B, and correspondingly cause the decline of activated GSDMD and GSDME. **(A&B)** The expression of caspase-8 and caspase-3 was knocked down by CRISPR- CAS9. **(C)** The cell viability of BEAS-2B were compared between control and caspase-8/3-KD cells after treatment with TNF-α and IFN-β for 72 h. **(D&E)** The activation of GSDMD and GSDME were compared between control and caspase-8/3-KD cells after treatment with TNF-α and IFN-β for 24 h and 48 h. The results are representative of at least three separate experiments. Data are shown as mean ± SEM. * $p < 0.05$, * * $p < 0.01$, * ** $p < 0.001$, * ** * $p < 0.0001$. Analysis was performed using the one-way ANOVA.

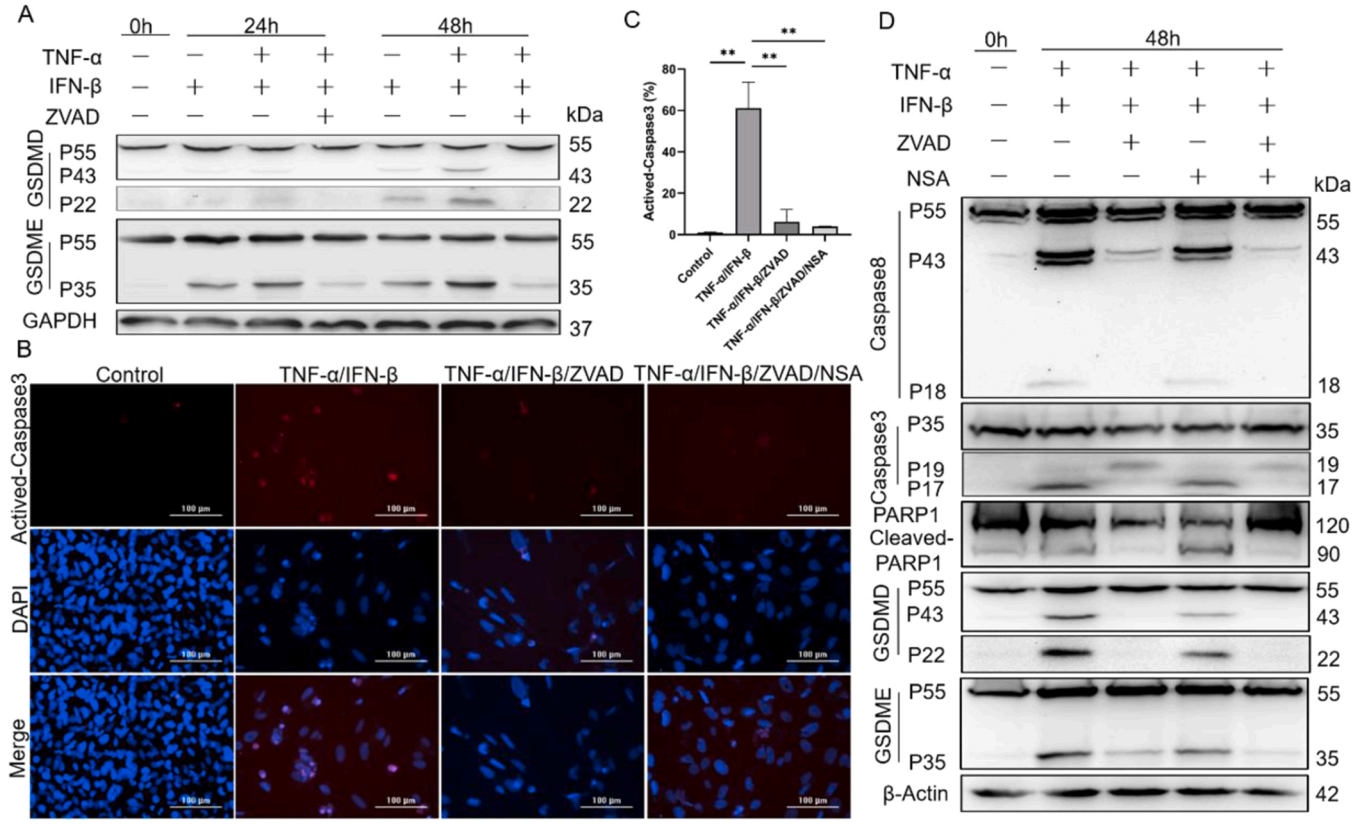

Fig. 7. TNF-α and IFN-β synergistically induce pyroptosis of BEAS-2B by activating both GSDMD and GSDME. **(A&D)** The cleavage and activation of caspase-8, caspase-3, PARP1, GSDMD and GSDME were analyzed by western blot after BEAS2B were treated as indicated for 24 and 48 h, respectively. **(B)** The fluorescence microscope images of BEAS-2B after cells were treated as indicated for 72 h. The red fluorescence indicates activated caspase-3 and the blue fluorescence indicates total cells. **(C)** The difference of activated caspase-3 between control and treated groups were quantified. Scale bar, 100 μm. The results are representative of at least three separate experiments. Data are shown as mean ± SEM. * * $p < 0.01$. Analysis was performed using the one-way ANOVA.

not be completely blocked by caspase inhibitors, compared to the cell death induced by TS, which almost were completely blocked by these inhibitors (Fig. 3F). These results prompted that TNF-α and IFN-β might induce other forms of cell death pathways besides apoptosis.

The cascade of necroptotic signals initiated by TNF-α is usually activated in the absence of caspase-8 activity and executed by RIPK3-phosphorylated MLKL (He et al., 2009; Sun et al., 2012). In our study, specific inhibitors were used to confirm whether TNF-α and IFN-β could synergistically trigger BEAS-2B necroptosis in the condition that caspase-8 activity was blocked by ZVAD. The results indicated that ZVAD did not intensify BEAS-2B death induced by TNF-α and IFN-β, as expected, and NSA, not RIPK-3 inhibitor GSK-872, blocked the cytotoxic effect of TNF-α and IFN-β when the enzymatic activity of caspase-8 was blocked with ZVAD, which prompted that it seemed that there was no necroptosis happening in TNF-α and IFN-β treated BEAS-2B (Fig. 4A-C). The western blot results further confirmed that co-treatment of TNF-α and IFN-β could not activate MLKL by phosphorylation, but promote the expression of MLKL (Fig. 4D). The function of increased MLKL in BEAS-2B induced by TNF-α and IFN-β deserved further investigation in the future. Given that the activation of MLKL is dependent on the expression and phosphorylation of RIPK3 (Pasparakis and Vandenabeele, 2015), the expression of RIPK3 in BEAS-2B was detected by western blot. The results indicated that BEAS-2B did not express RIPK3 (Fig. 4E), which might explain why TNF-α and IFN-β could not induce BEAS-2B to undergo necroptosis. Generally speaking, cancer cells do not express RIPK3 due to genomic methylation near its transcriptional start site, thus RIPK3-dependent activation of MLKL and downstream necroptosis are largely blocked in cancer cells (Fukasawa et al., 2006; Koo et al., 2015). According to our knowledge, it was seldom reported that normal tissue-derived cells did not express RIPK3. So the physiological function and related mechanism of RIPK3 silencing in normal cells, such as airway epithelial cells, deserve further investigation.

Pyroptosis is another form of proinflammatory cell death pathway initiated by activated caspases and characterized by increased release of LDH and IL-1β, and the presence of PI-positive cells and bubbles in the cell membrane of dying cells (Li et al., 2018; Wang et al., 2017). All these features of pyroptosis were found in TNF-α and IFN-β treated BEAS-2B in our experiment, except activation of caspase-1 (Figs. 2D, 3B, 5A-D). The combination of special inhibitors of caspase-8 and caspase-3 could partially improve the cells survival and reduce the release of LDH from BEAS-2B treated with TNF-α and IFN-β (Fig. 5E&F), which might be related to that caspase-8 and caspase-3 could initiate pyroptosis by activating GSDMD and GSDME (Sarhan et al., 2018; Wang et al., 2017). The decrease of activeated GSDMD and GSDME induced by TNF-α and IFN-β, and of the inhibitory effect of TNF-α and IFN-β on cell viability provided more direct support about this view, after the expression of caspase-8 and caspase-3 were knocked down in BEAS-2B (Fig. 6). The western blot results further confirmed that GSDMD and GSDME were cleaved into active fragments with the elongation of treatment time (Fig. 7A). At the same time, ZVAD could inhibit the activation of caspase-8 and caspase-3, and then the activation of GSDMD and GSDME, NSA had the inhibitory co-effect on the activation of GSDMD and GSDME with ZVAD (Fig. 7B-D). All these data indicated that there existed pyroptosis in TNF-α and IFN-β-treated BEAS-2B. In addition, NSA could not obviously block the activation of GSDMD and GSDME, but could inhibit TNF-α and IFN-β-induced BEAS-2B death alone or in combination with ZVAD (Figs. 3A, 4A, 7 D), which might be related to that NSA could directly bind Cys191 of activated GSDMD to inhibit its

oligomerization and the occurrence of pyroptosis (Rathkey et al., 2018).

Generally speaking, pyroptosis is triggered by the assembly and activation of inflammasomes and induced by inflammatory caspases, such as caspase-1/4/5 (Van Opdenbosch and Lamkanfi, 2019). Recently, it was reported that apoptotic casapse-8 and casapse-3 could also induce pyroptosis by cleaving GSDMD and GSDME, respectively (Sarhan et al., 2018; Wang et al., 2017) and our results also confirmed this conclusion. During pyroptosis, the cytokines and pathogens released from infected cells could recruit and activate immune cells to the site of infection, ultimately helping the host defend against invading pathogens. But the rapidly increased cytokines might also contribute to tissue damage and inflammatory disease (Man et al., 2017; Mandal et al., 2018). The function of IFN-β, which inhibited the replication of SARS-CoV-2 in airway epithelial cells on the one hand, and combined with TNF-α to induce airway epithelial cells death on the other hand, might reflect the double-edged sword feature of pyroptosis.

In conclusion, we first reported that the combination of TNF-α and IFN-β could induce airway epithelial cells BEAS-2B death. Furthermore, TNF-α and IFN-β mainly activated caspases-mediated apoptosis and GSDMs-mediated pyroptosis. At the same time, inhibiting activation of caspases and activity of GSDMs could block BEAS-2B death induced by TNF-α and IFN-β. These would provide insight for further elucidating the pathogenesis of COVID-19, and the development of targeted therapy for related viral infectious diseases.

Funding

This research was financially supported by the National Natural Science Foundation of China (81101730), the Basic and Applied Basic Research Fund of Guangdong Province (2020A1515110562), the Science and Technology Project of Guangzhou City (202102100003, 202102020092), the University Innovation and Entrepreneurship Education Project of Guangzhou (2020PT102) and the Student Innovation Promotion Program of Guangzhou Medical University (202266J056).

CRediT authorship contribution statement

R.S. and J.D. conceived and designed the study, performed experiments, and wrote the article. K.J., C.Z., R.Z., H.C., and H.L. performed experiments and analysis. All authors read and approved the final manuscript.

Declarations of interest

None.

Data Availability

Data will be made available on request.

References

Borczuk, A.C., Salvatore, S.P., Seshan, S.V., Patel, S.S., Bussel, J.B., Mostyka, M., et al., 2020. COVID-19 pulmonary pathology: a multi-institutional autopsy cohort from Italy and New York City. Mod. Pathol. 33 (11), 2156–2168. https://doi.org/10.1038/s41379-020-00661-1.

Chen, G., Goeddel, D. v, 2002. TNF-R1 signaling: a beautiful pathway. Science 296 (5573), 1634–1635. https://doi.org/10.1126/science.1071924.

Fukasawa, M., Kimura, M., Morita, S., Matsubara, K., Yamanaka, S., Endo, C., et al., 2006. Microarray analysis of promoter methylation in lung cancers. J. Hum. Genet 51 (4), 368–374. https://doi.org/10.1007/s10038-005-0355-4.

He, S., Wang, L., Miao, L., Wang, T., Du, F., Zhao, L., et al., 2009. Receptor interacting protein kinase-3 determines cellular necrotic response to TNF-α. Cell 137 (6), 1100–1111. https://doi.org/10.1016/j.cell.2009.05.021.

Huang, C., Wang, Y., Li, X., Ren, L., Zhao, J., Hu, Y., et al., 2020. Clinical features of patients infected with 2019 novel coronavirus in Wuhan, China. Lancet 395 (10223), 497–506. https://doi.org/10.1016/S0140-6736(20)30183-5.

Huys, L., van Hauwermeiren, F., Dejager, L., Dejonckheere, E., Lienenklaus, S., Weiss, S., et al., 2009. Type I interferon drives tumor necrosis factor-induced lethal shock. J. Exp. Med 206 (9), 1873–1882. https://doi.org/10.1084/jem.20090213.

Kaiser, W.J., Daley-Bauer, L.P., Thapa, R.J., Mandal, P., Berger, S.B., Huang, C., et al., 2014. RIP1 suppresses innate immune necrotic as well as apoptotic cell death during mammalian parturition. Proc. Natl. Acad. Sci. USA 111 (21), 7753–7758. https://doi.org/10.1073/pnas.1401857111.

Karki, R., Sharma, B.R., Tuladhar, S., Williams, E.P., Zalduondo, L., Samir, P., et al., 2021. Synergism of TNF-α and IFN-γ triggers inflammatory cell death, tissue damage, and mortality in SARS-CoV-2 infection and cytokine shock syndromes. e17 Cell 184 (1), 149–168. https://doi.org/10.1016/j.cell.2020.11.025.

Koo, G.B., Morgan, M.J., Lee, D.G., Kim, W.J., Yoon, J.H., Koo, J.S., et al., 2015. Methylation-dependent loss of RIP3 expression in cancer represses programmed necrosis in response to chemotherapeutics. Cell. Res. 25 (6), 707–725. https://doi.org/10.1038/cr.2015.56.

Lee, J.S., Shin, E.C., 2020. The type I interferon response in COVID-19: implications for treatment. Nat. Rev. Immunol. 20 (10), 585–586. https://doi.org/10.1038/s41577-020-00429-3.

Lee, J.S., Park, S., Jeong, H.W., Ahn, J.Y., Choi, S.J., Lee, H., et al., 2020. Immunophenotyping of COVID-19 and influenza highlights the role of type I interferons in development of severe COVID-19. Sci. Immunol. 5 (49), eabd1554. https://doi.org/10.1126/sciimmunol.abd1554.

Li, Y., Guo, X., Hu, C., Du, Y., Guo, C., Wang, D., et al., 2018. Type I IFN operates pyroptosis and necroptosis during multidrug-resistant A. baumannii infection. Cell. Death Differ. 25 (7), 1304–1318. https://doi.org/10.1038/s41418-017-0041-z.

Lucas, C., Wong, P., Klein, J., Castro, T.B.R., Silva, J., Sundaram, M., et al., 2020. Longitudinal analyses reveal immunological misfiring in severe COVID-19. Nature 584 (7821), 463–469. https://doi.org/10.1038/s41586-020-2588-y.

Major, J., Crotta, S., Llorian, M., McCabe, T.M., Gad, H.H., Priestnall, S.L., et al., 2020. Type I and III interferons disrupt lung epithelial repair during recovery from viral infection. Science 369 (6504), 712–717. https://doi.org/10.1126/science.abc2061.

Man, S.M., Karki, R., Kanneganti, T.D., 2017. Molecular mechanisms and functions of pyroptosis, inflammatory caspases and inflammasomes in infectious diseases. Immunol. Rev. 277 (1), 61–75. https://doi.org/10.1111/imr.12534.

Mandal, P., Feng, Y., Lyons, J.D., Berger, S.B., Otani, S., DeLaney, A., et al., 2018. Caspase-8 collaborates with caspase-11 to drive tissue damage and execution of endotoxic shock. e6 Immunity 49 (1), 42–55. https://doi.org/10.1016/j.immuni.2018.06.011.

Martines, R.B., Ritter, J.M., Matkovic, E., Gary, J., Bollweg, B.C., Bullock, H., et al., 2020. Pathology and pathogenesis of SARS-CoV-2 associated with fatal coronavirus disease, united states. Emerg. Infect. Dis. 26 (9), 2005–2015. https://doi.org/10.3201/eid2609.202095.

Meftahi, G.H., Jangravi, Z., Sahraei, H., Bahari, Z., 2020. The possible pathophysiology mechanism of cytokine storm in elderly adults with COVID-19 infection: the contribution of "inflame-aging. Inflamm. Res. 69 (9), 825–839. https://doi.org/10.1007/s00011-020-01372-8.

Mehta, P., McAuley, D.F., Brown, M., Sanchez, E., Tattersall, R.S., Manson, J.J., 2020. COVID-19: consider cytokine storm syndromes and immunosuppression. Lancet 395 (10299), 1033–1034. https://doi.org/10.1016/S0140-6736(20)30628-0.

Pasparakis, M., Vandenabeele, P., 2015. Necroptosis and its role in inflammation. Nature 517 (7534), 311–320. https://doi.org/10.1038/nature14191.

Rathkey, J.K., Zhao, J., Liu, Z., Chen, Y., Yang, J., Kondolf, H.C., et al., 2018. Chemical disruption of the pyroptotic pore-forming protein gasdermin D inhibits inflammatory cell death and sepsis. Sci. Immunol. 3 (26), eaat2738. https://doi.org/10.1126/sciimmunol.aat2738.

Sarhan, J., Liu, B.C., Muendlein, H.I., Li, P., Nilson, R., Tang, A.Y., et al., 2018. Caspase-8 induces cleavage of gasdermin D to elicit pyroptosis during Yersinia infection. Proc. Natl. Acad. Sci. U. S. A 115 (46), E10888–E10897. https://doi.org/10.1073/pnas.1809548115.

Silke, J., 2011. The regulation of TNF signalling: what a tangled web we weave. Curr. Opin. Immunol. 23 (5), 620–626. https://doi.org/10.1016/j.coi.2011.08.002.

Sun, L., Wang, H., Wang, Z., He, S., Chen, S., Liao, D., et al., 2012. Mixed lineage kinase domain-like protein mediates necrosis signaling downstream of RIP3 kinase. Cell 148 (1–2), 213–227. https://doi.org/10.1016/j.cell.2011.11.031.

Tracey, K.J., Beutler, B., Lowry, S.F., Merryweather, J., Wolpe, S., Milsark, I.W., et al., 1986. Shock and tissue injury induced by recombinant human cachectin. Science 234 (4775), 470–474. https://doi.org/10.1126/science.3764421.

Van Opdenbosch, N., Lamkanfi, M., 2019. Caspases in cell death, inflammation, and disease. Immunity 50 (6), 1352–1364. https://doi.org/10.1016/j.immuni.2019.05.020.

Vanderheiden, A., Ralfs, P., Chirkova, T., Upadhyay, A.A., Zimmerman, M.G., Bedoya, S., et al., 2020. Type I and Type III Interferons Restrict SARS-CoV-2 Infection of Human Airway Epithelial Cultures. e00985–20 J. Virol. 94 (19). https://doi.org/10.1128/jvi.00985-20.

Walczak, H., 2011. TNF and ubiquitin at the crossroads of gene activation, cell death, inflammation, and cancer. Immunol. Rev. 244 (1), 9–28. https://doi.org/10.1111/j.1600-065x.2011.01066.x.

Wang, J., Jiang, M., Chen, X., Montaner, L.J., 2020. Cytokine storm and leukocyte changes in mild versus severe SARS-CoV-2 infection: review of 3939 COVID-19 patients in China and emerging pathogenesis and therapy concepts. J. Leukoc. Biol. 108 (1), 17–41. https://doi.org/10.1002/JLB.3COVR0520-272R.

Wang, Y., Gao, W., Shi, X., Ding, J., Liu, W., He, H., et al., 2017. Chemotherapy drugs induce pyroptosis through caspase-3 cleavage of a gasdermin. Nature 547 (7661), 99–103. https://doi.org/10.1038/nature22393.

WHO Coronavirus (COVID-19) Dashboard. ⟨https://covid19.who.int/⟩. (accessed 17 June 2022).